NANO EXPRESS

TiO$_2$/Porous Carbon Composite-Decorated Separators for Lithium/Sulfur Battery

Haisheng Han[1], Songqiao Niu[1], Yan Zhao[1*], Taizhe Tan[2] and Yongguang Zhang[1*]

Abstract

The practical application of lithium/sulfur (Li/S) batteries is hindered by the migration of soluble polysulfides (Li$_2$S$_n$, $4 \leq n \leq 8$) from cathode to anode, leading to poor electrochemical stability of the cell. To address this issue, in the present study, a TiO$_2$/porous carbon (TiO$_2$/PC) composite-coated Celgard 2400 separator was successfully fabricated and used as a polysulfide barrier for the Li/S battery. In TiO$_2$/PC, the highly conductive PC with three-dimensional ordered porous structure physically constrains polysulfides and at the same time serves as an additional upper current collector. On the other hand, the TiO$_2$ on the surface of PC chemically adsorbed polysulfides during the charge/discharge process. Due to the physical and chemical adsorption properties of TiO$_2$/PC composite coating layer, an initial discharge capacity of 926 mAh g^{-1} at 0.1 C and a low fading rate (75% retention after 150 cycles) were achieved. Moreover, in the rate capability test, the discharge capacity for the TiO$_2$/PC-modified Li/S battery was recovered to 728 mAh g^{-1} at 0.1 C after high-rate cycling and remained ~ 88% of the initial reversible capacity.

Keywords: TiO$_2$-decorated porous carbon, Modified separator, Lithium/sulfur battery, Polysulfide barrier

Background

Among the rechargeable batteries, lithium/sulfur (Li/S) battery has been considered as a promising candidate for the next-generation power supplies because of their high theoretical energy density (2600 Wh kg^{-1}) and specific capacity (1675 mAh g^{-1}) [1]. Additionally, Li/S batteries also have other advantageous features such as low toxicity, low cost, and high natural abundance [2].

However, there are still some problems hindering the practical application of Li/S batteries. These problems include the following: (i) the insulating nature of elemental sulfur ($\sigma_{298} = 5 \times 10^{-30}$ S cm^{-1}) would result in the low utilization of the active material; (ii) the volume change resulting from the different volume density of Li$_2$S and sulfur leads to a serious capacity decay of the battery; and (iii) the dissolution and diffusion of polysulfides in the electrolyte would cause a low Coulombic efficiency and rapid decline in the capacity [3, 4].

To solve these problems, extensive efforts have been devoted to confine S within the cathode region [5, 6]. A large number of materials such as porous carbon,

inorganic oxides, and polymers have been designed and synthesized to trap the polysulfide within the cathodes [7–13]. However, the introduction of high content sulfur-trapping materials inevitably reduces the overall energy densities of the cell. Therefore, various strategies beyond the cathode modification have been explored.

An alternative strategy to suppress the dissolution and diffusion of polysulfides is the modification of the internal structure of the Li/S battery, such as building a coating interlayer on the separator [14, 15]. Thus, different kinds of carbon-based modified separators are widely applied to Li/S batteries to inhibit the diffusion of polysulfides though physical absorption [16, 17]. Li et al. groups reported the reduced graphene oxide/active carbon functional interlayer could improve the cycle performance of Li/S battery [17]. Nevertheless, the weak interaction between the unpolar carbon matrix and polar polysulfides is considered to be insufficient to immobilize the migrating polysulfides. Therefore, carboneous materials are usually composited with the polar metal oxides, such as layered double hydroxide, CeO$_2$, which could offer a stronger chemical binding to polysulfides through polar-polar interaction [18–22]. The chemical nature between polysulfides and polar TiO$_2$ surface and carbon

* Correspondence: yanzhao1984@hebut.edu.cn;
yongguangzhang@hebut.edu.cn
[1]School of Materials Science and Engineering, Hebei University of Technology, Tianjin 300130, China
Full list of author information is available at the end of the article

Han *et al. Nanoscale Research Letters* (2019) 14:176

Page 2 of 8

functional groups has been well-demonstrated both experimentally and theoretically [23, 24].

Herein, we reported a TiO_2-decorated porous carbon (TiO_2/PC) as a coating layer on Celgard 2400 separator to suppress the polysulfide shuttle effect. In the TiO_2/PC composite, TiO_2 nanoparticles uniformly decorated on the surface of PC could effectively restrain the diffusion of polysulfides by chemical bonding. On the other hand, the PC layer not only ensures the good electrical conductivity of the composite, but also can mitigate the polysulfides dissolution by providing a physical confinement of polysulfides within its porous structure.

Methods
Preparation of Li/S Battery with TiO_2/PC-Modified Separator
Preparation of Porous Carbon
Figure 1 displays the schematic representation of the fabrication process of the TiO_2/PC-modified Celgard 2400 separator. Monodisperse silica microspheres were first prepared by hydrolyzing tetraethyl orthosilicate (TEOS) with an ammonia solution and then centrifugally dispersed in ethanol. The ethanol solution was naturally dried to obtain silica opal, which was then dispersed in a resol solution. Here, resol was used as a carbon source and was treated at 600 °C for 2 h under argon atmosphere with a heating ramp of 2 °C min^{-1} in a tube furnace. An 11% weight loss in the carbonization of resol was observed. Then, the silica opal template was etched by HF

solution, and the PC template with ordered porous structure was obtained.

Deposition of TiO_2 on PC
The TiO_2 presoma solution was prepared by a sol–gel method. First, 2.84 g (0.1 mol) of tetraisopropyl titanate (TTIP), 2.4 g of hydrochloric acid, and 4.0 g of ethylalcohol were mixed and stirred for 1.5 h to form a transparent gel solution. The PC template was soaked in the TiO_2 solution for 24 h. Then, the PC template deposited with TiO_2 was collected and naturally dried for 3 days. After that, it was heat treated at 450 °C for 1 h under N_2 atmosphere for further use.

Preparation of the TiO_2/PC-Modified Separator
A slurry was prepared by mixing 0.7 g TiO_2/PC, 0.2 g carbon black, and 0.1 g polyvinylidene difluoride (PVDF) in N-methyl pyrrolidone (NMP) solvent. The slurry was coated onto the commercial Celgard 2400 separator and dried at 50 °C overnight in a vacuum drying oven. The thickness of TiO_2/PC on Celgard 2400 separator is 37 μm, and the areal loading of TiO_2/PC is about 0.5 mg cm^{-2}. The TiO_2/PC-modified Celgard 2400 separator was cut into disks of 1 cm in diameter.

Material Characterizations
The crystalline structure of the TiO_2/PC-modified separator was measured by using powder X-ray diffraction (XRD, Smart Lab, Rigaku), with Cu–Kα radiation ($\lambda = 1.5406$ Å) at the 2θ range of 10 to 90°. The
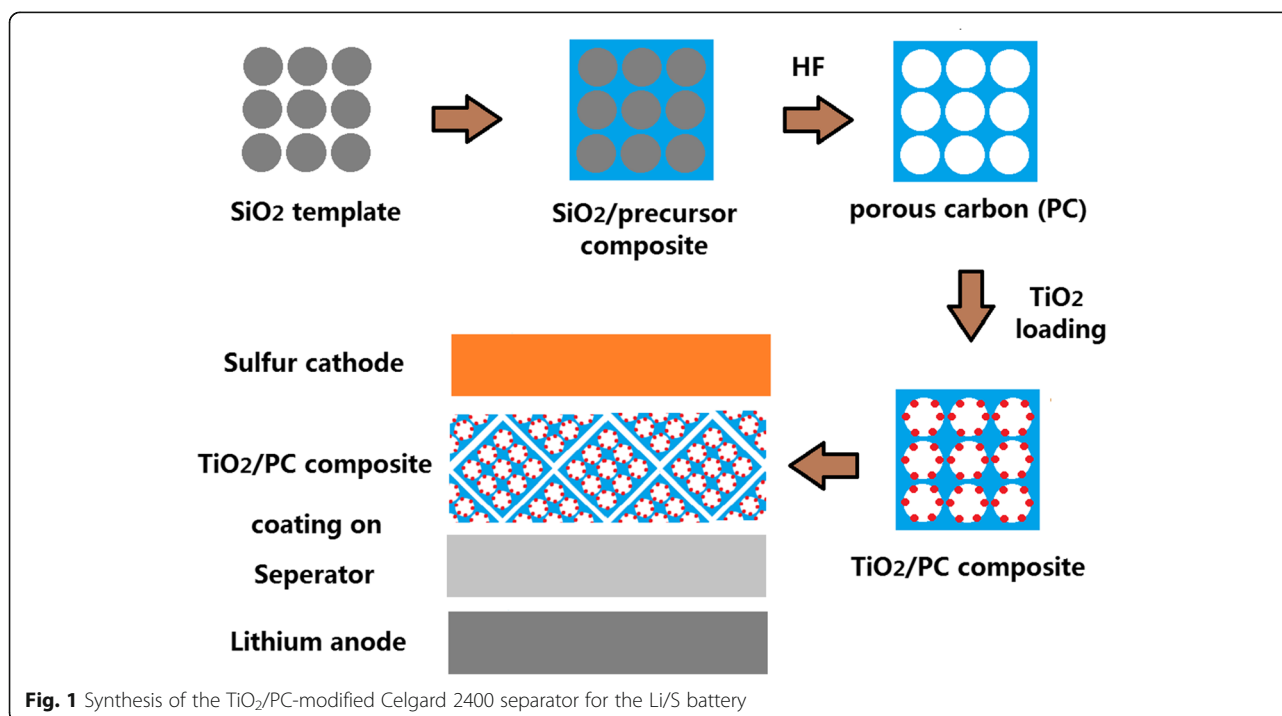

Fig. 1 Synthesis of the TiO_2/PC-modified Celgard 2400 separator for the Li/S battery

Han *et al. Nanoscale Research Letters*   (2019) 14:176

Page 3 of 8

morphology of the obtained TiO$_2$/PC composite was studied by scanning electron microscopy (SEM, JSM-7100F, JEOL) and transmission electron microscopy (TEM, JEM-2100F, JEOL) with an accelerated voltage of 200 kV (Additional file 1). The contact angle measurement was performed using an JGW-360Y contact angle meter. The functional groups of the TiO$_2$/PC-modified separator after charge/discharge were tested by using X-ray photoelectron spectroscopy (XPS, Kratos AXIS Ultra DLD, Al–Kα).

Electrochemical Measurements

The slurry of the sulfur cathode was prepared by mixing 0.8 g S, 0.1 g carbon black, and 0.1 g PVDF in NMP. The slurry was coated onto Al foil and dried at 60 °C overnight under vacuum condition. The sulfur electrodes were then cut into 1-cm disks. The sulfur loading is approximately 2.0 mg cm^{-2}. The amount of electrolyte is around 40 μL. Metallic Li was used as the anode, and the electrolyte used was 1 M LiTFSI in a binary dioxolane (DOL) and dimethoxyethane (DME) solvent (1:1 v/v). The electrochemical performance was evaluated by coin cells (CR2025) which were assembled in an MBraun glove box under high-purity argon (Ar ≥ 99.9995%). The electrochemical charge/discharge performance was measured between 1.5 and 3 V with a Neware battery tester (BTS-5V5mA) at room temperature.

Results and Discussion

Figure 2 shows the XRD pattern for the TiO$_2$/PC-modified separator. The crystalline phase was identified as anatase TiO$_2$ (JCPDS No.21-1272). Additionally, there were two typical peaks at around 23° and 44°, corresponding to the diffraction from (002) and (100) of carbon, respectively.
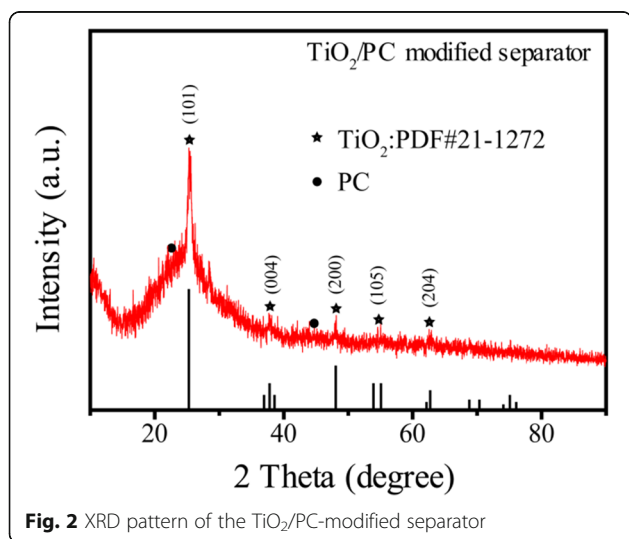

Fig. 2 XRD pattern of the TiO$_2$/PC-modified separator

Figure 3 shows the SEM and TEM results for TiO$_2$/PC. Figure 3a–c clearly show the uniform ordered porous structure of TiO$_2$/PC with a pore size of ~ 110 nm in diameter. The TiO$_2$ nanoparticles were evenly distributed in the PC. Figure 3 d shows a lattice spacing of 0.35 nm which corresponds to the (101) facet of anatase TiO$_2$ and further illustrates the TiO$_2$ nanoparticles were uniformly dispersed in the PC.

Figure 4a shows the nitrogen adsorption–desorption isotherms of the TiO$_2$/PC with a BET surface area of 263 m^2 g^{-1}. The pore diameter distribution curve shows the as-prepared TiO$_2$/PC composite is composed of small-size micropores around 1 nm (inset) and a relatively broad mesoporous distribution, see Fig. 4b.

Figure 5a demonstrates the XPS survey spectrum of the TiO$_2$/PC-modified separator after charge/discharge, confirming the presence of O, Ti, C, and S in TiO$_2$/PC. Figure 5b–d shows the high-resolution XPS spectra of C 1s, S 2p, and Ti 2p. In Fig. 5b, the two peaks in C 1s spectrum can be assigned to two different carbon-containing functional groups, C–C/C=C (284.6 eV) and O–C=O (290.4 eV). In the S 2p spectrum, the weak peak at 162.90 eV corresponds to the S–Ti bond [25, 26], while the three weak peaks at 163.9, 165.0, and 170.40 eV correspond to S 2p$_{2/3}$, S 2p$_{1/2}$, and the sulfate, respectively (Fig. 5c) [27]. The strong peaks located at 167.0 and 169.0 eV correspond to the –SO$_3$ and C–S bonds, respectively [28, 29]. The three peaks found in Fig. 5d at 458.25, 459, and 464.7 eV represent Ti–S, Ti 2p$_{2/3}$, and Ti 2p$_{1/2}$, respectively. The presence of a Ti–S bond in the high-resolution XPS spectra of Ti 2p and S 2p reveals the presence of a chemical bond between the elemental sulfur and TiO$_2$.

Figure 6 a shows the excellent flexibility of the TiO$_2$/PC-modified separator. Contact angle measurement was employed to examine the infiltration ability of the electrolyte solution through the TiO$_2$/PC-modified separator. Figure 6b shows the contact angle of the electrolyte on the surface of the unmodified separator was 37.98°, while for the TiO$_2$/PC-modified separator, it was 0°. This result implies that the TiO$_2$/PC coating on the separator improved the electrolyte infiltration due to the polar nature of porous TiO$_2$/PC composite.

The cyclic voltammetry (CV) curves of the Li/S batteries with and without TiO$_2$/PC-modified separators were measured at a scan rate of 0.1 mV s^{-1}. Both the Li/S batteries exhibit two main cathodic peaks and one anodic peak in Fig. 7. The Li/S battery with TiO$_2$/PC-modified separator presents a higher potential cathodic peak at 2.27 V and a relatively lower potential cathodic peak at 1.97 V, corresponding to the reduction of sulfur to soluble polysulfides (Li$_2$S$_n$, $4 \leq n \leq 8$) and then further reduction to Li$_2$S/Li$_2$S$_2$, respectively. The major anodic peak at 2.44 V is ascribed to the conversion of Li$_2$S/Li$_2$S$_2$ to sulfur. Compared to the Li/S battery with
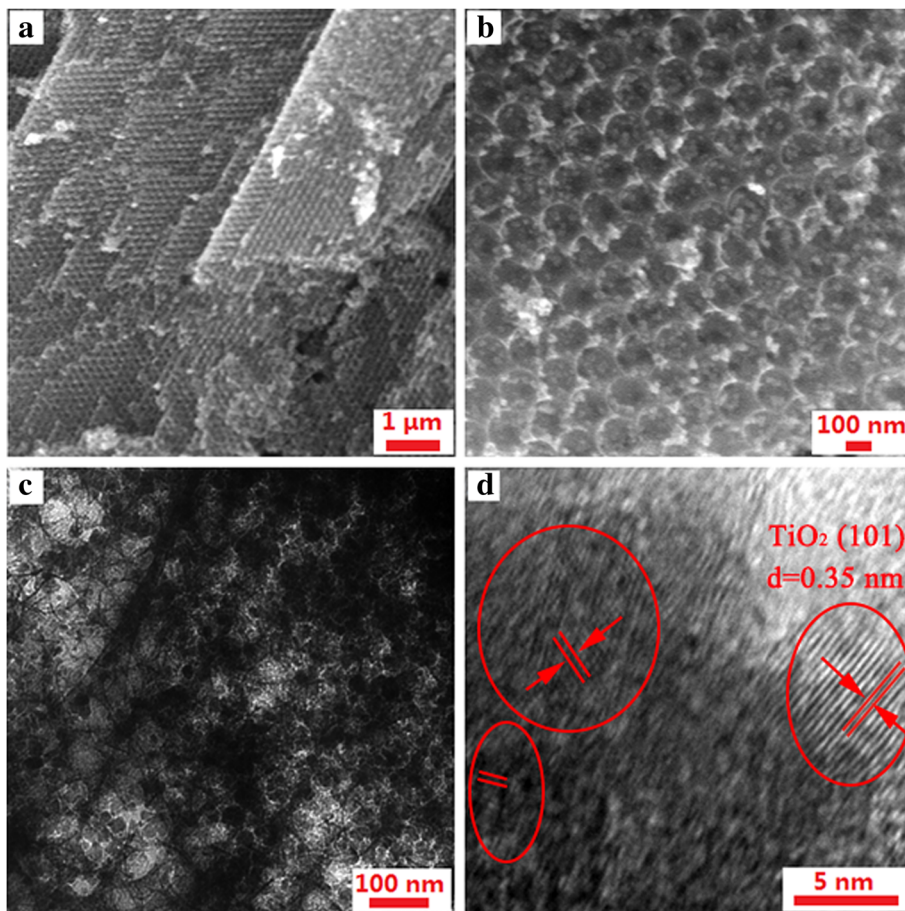
Fig. 3 SEM (**a**, **b**) and TEM (**c**, **d**) images of the TiO$_2$/PC interlayer

pristine separator, the Li/S battery with TiO$_2$/PC-modified separator delivers the higher potential cathodic peaks and the smaller potential anodic peak, which indicates that the TiO$_2$/PC-modified separator effectively suppresses the potential polarization and enhances the electrochemical kinetics of Li/S batteries.

The galvanostatic charge/discharge curves for the Li–S cell with TiO$_2$/PC-modified Celgard 2400 separator measured at 0.1 C were shown in Fig. 8. Two typical discharge plateaus were observed at 2.27 and 1.97 V, which can be ascribed to the two-step reaction between S and Li. The first plateau can be ascribed
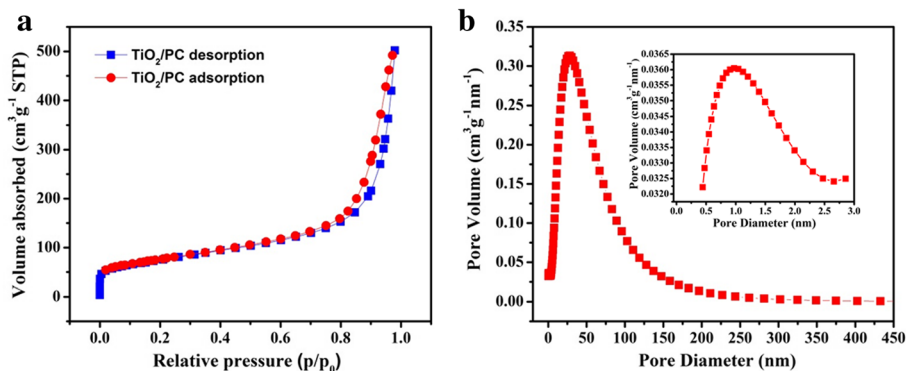

Fig. 4 a N$_2$ adsorption–desorption isotherms. **b** Pore diameter distribution of TiO$_2$/PC. Inset: magnification of pore diameter distribution between 0 and 3 nm
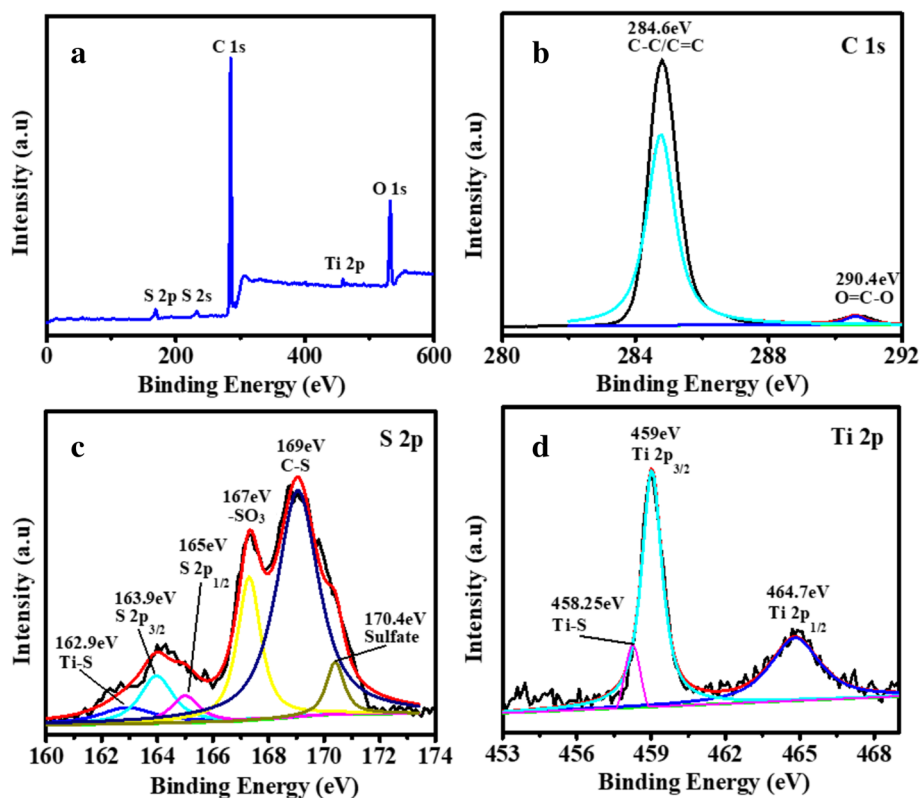
Fig. 5 Wide spectrum (**a**) and high-resolution XPS spectra of the TiO₂/PC-modified separator after charge/discharge spectra of C 1s, S 2p, and Ti 2p (**b**–**d**)

to the reduction of the S_8 and the formation of S_8^{2-}, and the second plateau is related to the reaction of Li_2S_n, $(4 \leq n \leq 8)$ to Li_2S_2 and Li_2S [30, 31]. The plateaus during the initial three charge/discharge cycles were presented. The initial discharge capacity was 1060 mAh g^{-1} at 0.1 C. In the second and third cycles, the reversible capacities of 926 mAh g^{-1} and 853 mAh g^{-1}, respectively, were achieved, suggesting a good cyclability of the Li–S cell.

The cycling performance of the cell with TiO₂/PC-modified Celgard 2400 separator was investigated. Figure 9 shows that, at 0.1 C, the cell delivers an initial capacity of 1060 mAh g^{-1} and an reversible capacity of 926 mAh g^{-1}. After 150 cycles, the battery remains at ~
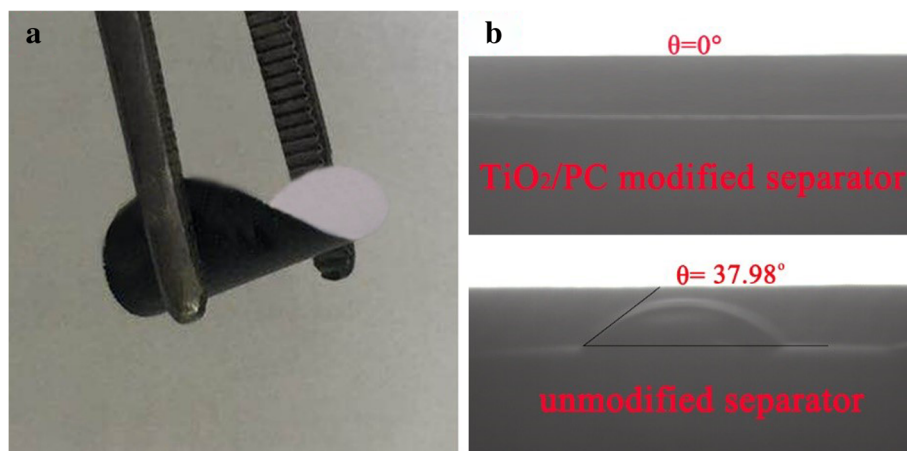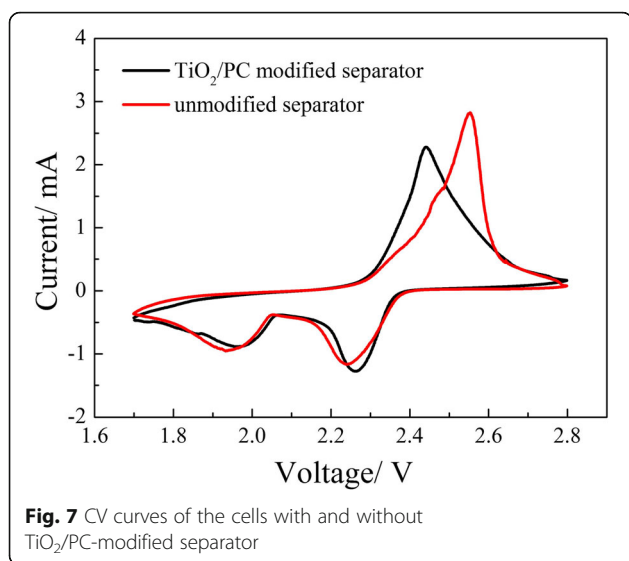

Fig. 6 Digital images of the TiO₂/PC-modified separator with excellent flexibility. (**a**) The contact angle of the electrolyte on the surface of the TiO₂/PC-Modified separator and the unmodified separator (**b**)

Han et al. Nanoscale Research Letters   (2019) 14:176

Page 6 of 8

Fig. 7 CV curves of the cells with and without TiO₂/PC-modified separator

Fig. 9 Cycling stability of the cell (with TiO₂/PC-modified separator and unmodified) at 0.1 C
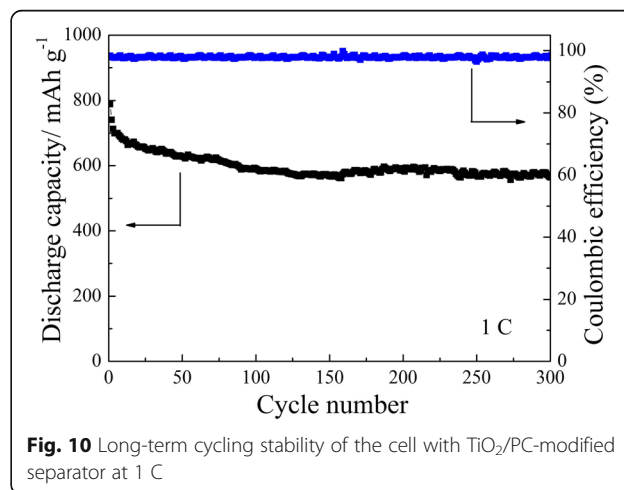
75% of the initial reversible capacity (708 mAh g^{-1}). On the other hand, the cell with unmodified Celgard 2400 separator shows a lower discharge capacity and a poor cycling performance, indicating that the TiO₂/PC-modified separator could effectively absorb polysulfides and suppress the shuttle effect. The prolonged cycling life of the cell with TiO₂/PC-modified Celgard 2400 separator was measured at 1 C (Fig. 10). It delivers an initial discharge capacity of 788 mAh g^{-1} and remains a very stable stability with a reversible capacity of 564 mAh g^{-1} after 300 cycles, which delivers a superior electrochemical performance.
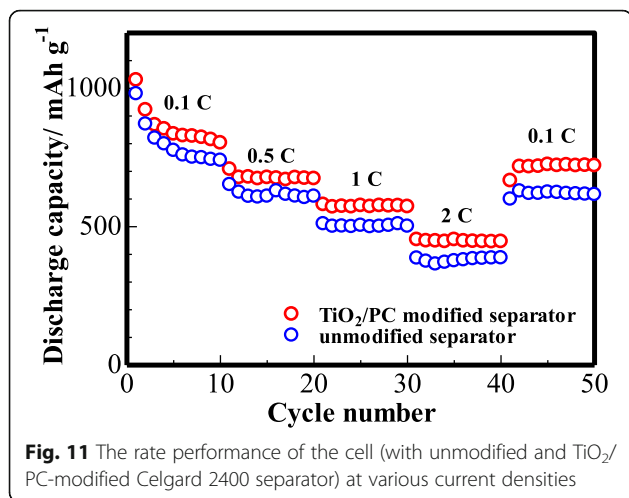
To further investigate the rate capability of the modified cell, a rate performance test was performed (Fig. 11). One can see that the battery with modified Celgard 2400 separator shows reversible capacities of around 823, 672, 578, and 455 mAh g^{-1} at the rate of 0.1, 0.5, 1, and 2 C,
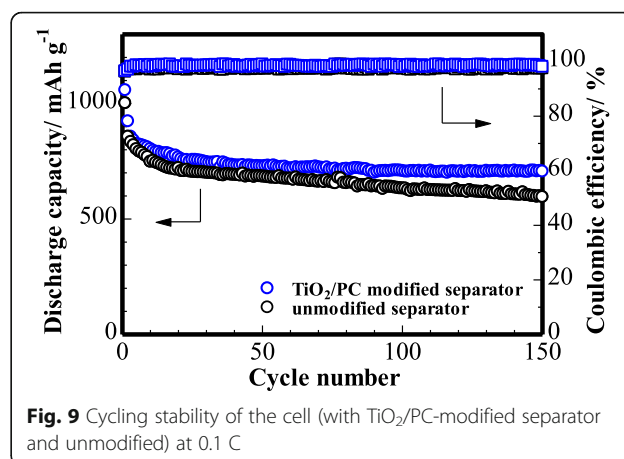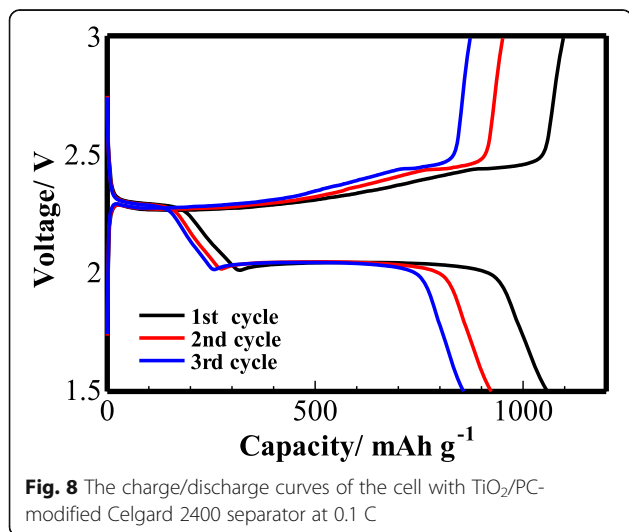
respectively. Meanwhile, the discharge capacity could recover to 728 mAh g^{-1} at 0.1 C and remained at ~ 88% of the initial reversible capacity after high-rate cycling, revealing a good capacity recovery. Nevertheless, the battery with unmodified separator exhibits a lower capacity at different current rates. The results further demonstrate that the cell with TiO₂/PC-modified separator can enhance S utilization and inhibit the polysulfide's diffusion.

The polysulfide's diffusion in electrolyte solution results in the self-discharge behavior of the cells. The Li–S batteries with modified and unmodified separator were left to stand (72 h) after the initial 3 cycles at 0.1 C and then tested for further charge/discharge. Figure 12 shows the open-circuit voltage curve for the battery with unmodified separator. It displays an obvious voltage decrease of 0.21 V (2.28~2.07 V) during the rest time, indicating a serious self-reduction process from high-order to low-order polysulfides [32]. Nevertheless, the self-discharge voltage of the cell with TiO₂/PC-modified separator exhibits only 2.6% decrease of the original open-circuit voltage
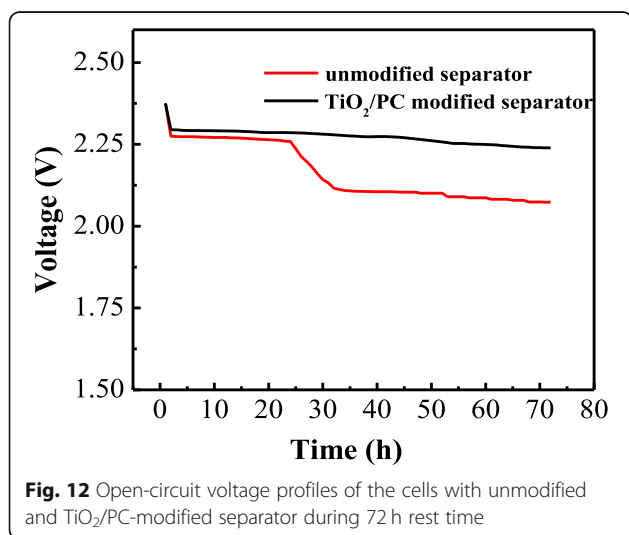

Fig. 8 The charge/discharge curves of the cell with TiO₂/PC-modified Celgard 2400 separator at 0.1 C

Fig. 10 Long-term cycling stability of the cell with TiO₂/PC-modified separator at 1 C

Han *et al. Nanoscale Research Letters*   (2019) 14:176

Page 7 of 8

Fig. 11 The rate performance of the cell (with unmodified and TiO$_2$/PC-modified Celgard 2400 separator) at various current densities

(2.3~2.24 V) during the rest time, demonstrating that the TiO$_2$/PC-modified separator can effectively alleviate the self-discharge of Li–S cell.

Conclusions

In summary, a TiO$_2$/PC-modified Celgard 2400 separator was successfully synthesized for Li/S battery, which can effectively enhance the electrochemical properties of the battery. TiO$_2$ could suppress the shuttle effect via electrostatic attraction (S–Ti–O). Meanwhile, the PC in the composite not only enhances the electrical conductivity of the separator, but also inhibits the polysulfide's diffusion by providing a physical confinement effect within its ordered porous structure. As a result, a high initial specific capacity of 926 mAh g^{-1} is achieved, together with a good cycling stability over 150 cycles. This work provides an effective approach for separator modification for high-performance Li/S batteries.

Fig. 12 Open-circuit voltage profiles of the cells with unmodified and TiO$_2$/PC-modified separator during 72 h rest time

Additional File

Additional file 1: Figure S1. The cross-section SEM image of TiO$_2$/PC on Celgard 2400 separator. **Figure S2.** The cycled SEM image of the TiO$_2$/PC modified separator. (DOC 607 kb)

Abbreviations
DME: 1,2-Dimethoxyethane; DOL: 1,3-Dioxolane; Li/S: Lithium/sulfur; LiTFSI: Lithium bis (trifluoromethanesulfonyl)imide; NMP: *N*-methyl pyrrolidone; PC: Porous carbon; PVDF: Polyvinylidene fluoride; SEM: Scanning electron microscope; TEM: Transmission electron microscope; TEOS: Hydrolyzing tetraethyl orthosilicate; TiO$_2$: Titanium dioxide; TTIP: Tetraisopropyl titanate; XPS: X-ray photoelectron spectroscopy; XRD: X-ray diffraction

Availability of Data and Materials
All data generated or analyzed during this study are included in this published article.

Authors' Contributions
YGZ conceived and designed the experiments. HH and SN carried out the experiments. HH and TT analyzed the data. TT, HH, and YZ drafted and revised the manuscript. YZ and YGZ supervised the work and finalized the manuscript. All authors read and approved the final manuscript.

Competing Interests
The authors declare that they have no competing interests.

Publisher's Note
Springer Nature remains neutral with regard to jurisdictional claims in published maps and institutional affiliations.

Author details
[1]School of Materials Science and Engineering, Hebei University of Technology, Tianjin 300130, China. [2]Synergy Innovation Institute of GDUT, Heyuan, Guangdong Province, China.

References
1. Jin J, Wen Z, Ma G, Lu Y, Rui K (2014) Mesoporous carbon/sulfur composite with polyaniline coating for lithium sulfur batteries. Solid State Ionics 262:170–173
2. Li XG, Rao M, Chen DR, Lin HB, Liu YL, Liao YH, Xing LD, Li WS (2015) Sulfur supported by carbon nanotubes and coated with polyaniline: preparation and performance as cathode of lithium-sulfur cell. Electrochim Acta 166:93–99
3. Zhang Y, Zhao Y, Bakenov Z (2014) A novel lithium/sulfur battery based on sulfur/graphene nanosheet composite cathode and gel polymer electrolyte. Nanoscale Res Lett 9:137–144
4. Choi YJ, Chung YD, Baek CY, Kim KW, Ahn HJ, Ahn JH (2008) Effects of carbon coating on the electrochemical properties of sulfur cathode for lithium/sulfur cell. J Power Sources 184:548–552
5. Wang X, Zhang Z, Qu Y, Lai Y, Li J (2014) Nitrogen-doped graphene/sulfur composite as cathode material for high capacity lithium-sulfur batteries. J Power Sources 256:361–368
6. Li XL, Cao YL, Qi W, Saraf LV, Xiao J, Nie ZM, Mietek J, Zhang JG, Schwenzera B, Liu J (2011) Optimization of mesoporous carbon structures for lithium-sulfur battery applications. J Mater Chem 21:16603–16610
7. Elazari R, Salitra G, Garsuch A, Panchenko A, Aurbach D (2011) Sulfur-impregnated activated carbon fiber cloth as a binder-free cathode for rechargeable Li-S batteries. Adv Mater 23:5641–5644

8. Xu JT, Shui JL, Wang JL, Wang M, Liu HK, Dou SX, Jeon IY, Seo JM, Baek JB, Dai LM (2014) Sulfur-graphene nanostructured cathodes via ball-milling for high-performance lithium-sulfur batteries. ACS Nano 8:10920–10930
9. Xi K, Kidambi PR, Chen R, Gao C, Peng X, Ducati C, Hofmann S, Kumar RV (2014) Binder free three-dimensional sulphur/few-layer graphene foam cathode with enhanced high-rate capability for rechargeable lithium sulphur batteries. Nanoscale 6:5746–5753
10. Sun Z, Wang S, Yan L, Xiao M, Han D, Meng Y (2016) Mesoporous carbon materials prepared from litchi shell as sulfur encapsulator for lithium-sulfur battery application. J Power Sources 324:547–555
11. Zhou G (2012) Flexible nanostructured sulfur-carbon nanotube cathode with high-rate performance for Li-S batteries. Energy Environ Sci 5:8901–8906
12. Zhang CF, Wu HB, Yuan C, Guo Z, Lou XW (2012) Confining sulfur in double-shelled hollow carbon spheres for lithium-sulfur batteries. Angew Chem 124:9594–9594
13. Zhang Y, Zhao Y, Bakenov Z, Tuiyebayeva M, Konarov A, Chen P (2014) Synthesis of hierarchical porous sulfur/polypyrrole/multiwalled carbon nanotube composite cathode for lithium batteries. Electrochim Acta 143:49–55
14. Zhou GM, Pei SF, Li L, Wang DW, Wang SG, Huang K, Yin LC, Li F, Cheng HM (2014) A graphene-pure-sulfur sandwich structure for ultrafast, long-life lithium-sulfur batteries. Adv Mater 26:625–631
15. Shao H, Wang W, Zhang H, Wang A, Chen X, Huang Y (2018) Nano-TiO_2 decorated carbon coating on the separator to physically and chemically suppress the shuttle effect for lithium-sulfur battery. J Power Sources 378:537–545
16. Su YS, Manthiram A (2012) Lithium-sulphur batteries with a microporous carbon paper as a bifunctional interlayer. Nat Commun 3:1166–1171
17. Li H, Sun L, Zhang Y, Tan T, Wang G, Bakenov Z (2017) Enhanced cycle performance of Li/S battery with the reduced graphene oxide/activated carbon functional interlayer. J Energy Chem 26:1276–1281
18. Pang Q, Kundu D, Cuisinier M, Nazar LF (2014) Surface-enhanced redox chemistry of polysulphides on a metallic and polar host for lithium-sulphur batteries. Nat Commun 5:4759–4766
19. Huang JQ, Zhang Q, Wei F (2015) Multi-functional separator/interlayer system for high-stable lithium-sulfur batteries: progress and prospects. Energy Storage Mater 1:127–145
20. Peng HJ, Zhang ZW, Huang JQ, Zhang G, Xie J, Xu WT, Shi JL, Chen X, Cheng XB, Zhang Q (2016) A cooperative interface for highly effcient lithium–sulfur batteries. Adv Mater 28:9551–9558
21. Wang SY, Gao F, Zhao Y, Liu N, Tan TZ, Wang X (2018) Two-dimensional CeO_2/RGO composite-modified separator for lithium/sulfur batteries. Nanoscale Res Lett 13:377
22. Liang X, Kwok CY, Lodi-Marzano F, Pang Q, Cuisinier M, Huang H, Hart CJ, Houtarde D, Kaup K, Sommer H, Brezesinski T, Janek J, Nazar LF (2016) Tuning transition metal oxide-sulfur interactions for long life lithium sulfur batteries: the "Goldilocks" principle. Adv Energy Mater 6:1501636
23. Zu CX, Dolocan A, Xiao PH, Stauffer S, Henkelman G, Manthiram A (2016) Breaking down the crystallinity: the path for advanced lithium batteries. Adv Energy Mater 6:1501933
24. Klein MJ, Dolocan A, Zu CX, Manthiram A (2017) An effective lithium sulfide encapsulation strategy for stable lithium-sulfur batteries. Adv Energy Mater 7:1701122
25. Lin T, Yang C, Wang Z, Yin H, Lu XJ, Huang FQ, Lin JH, Xie XM, Jiang MH (2014) Effective nonmetal incorporation in black titania with enhanced solar energy utilization. Energy Environ Sci 7:967–972
26. Tu W, Zhou Y, Feng S, Xu Q, Li P, Wang X, Xiao M, Zou Z (2015) Hollow spheres consisting of $Ti_{0.91}O_2$/CdS nanohybrids for CO_2 photofixation. Chem Commun 51:13354–13357
27. Li YY, Cai QF, Wang L, Li QW, Peng X, Gao B, Huo KF, Chu PK (2016) Mesoporous TiO_2 nanocrystals/graphene as an efficient sulfur host material for high-performance lithium-sulfur batteries. ACS Appl Mater Inter 8:23784–23792
28. Gao L, Cao ML, Fu YQ, Zhong ZC, Shen Y, Wang MK (2016) Hierarchical TiO_2 spheres assisted with graphene for high performance lithium-sulfur battery. J Mater Chem A 4:16454–16461
29. Lindberg BJ, Hamrin K, Johansson G, Gelius U, Fahlmann A, Nordling C, Siegbahn K (1970) Molecular spectroscopy by means of ESCA II: sulfur compounds, correlation of electron binding energy with structure. Phys Scr 1:288–298
30. Yang ZZ, Wang HY, Lu L, Wang C, Zhong XB, Wang JG, Jiang QC (2016) Hierarchical TiO_2 spheres as highly efficient polysulfide host for lithium-sulfur batteries. Sci Rep 6:22990–22997
31. Yu MP, Ma JS, Song HQ, Wang AJ, Tian FY, Wang YS, Qiu H, Wang RM (2016) Atomic layer deposited TiO_2 on a nitrogen-doped graphene/sulfur electrode for high performance lithium-sulfur batteries. Energy Environ Sci 9:1495–1503
32. Huang JQ, Zhuang TZ, Zhang Q, Peng HJ, Chen CM, Wei F (2015) Permselective graphene oxide membrane for highly stable and anti-self-discharge lithium-sulfur batteries. ACS Nano 9:3002–3011